1989ApJ...339...84M

THE ASTROPHYSICAL JOURNAL, 339:84–92, 1989 April 1
© 1989. The American Astronomical Society. All rights reserved. Printed in U.S.A.

THE AGE OF THE LMC GLOBULAR CLUSTER NGC 1783

JEREMY MOULD[1]
Palomar Observatory, California Institute of Technology
JEROME KRISTIAN
Mount Wilson and Las Campanas Observatory
JAMES NEMEC
Caltech and University of British Columbia
MARC AARONSON[1,2]
Steward Observatory, University of Arizona
AND
JOSEPH JENSEN
California Institute of Technology
Received 1988 June 15; accepted 1988 September 1

ABSTRACT

The age of the LMC red globular cluster NGC 1783 is estimated as 0.9 ± 0.4 billion yr by photometry of the main-sequence turnoff. The accuracy of the estimate is limited chiefly by uncertainty in the distance modulus of the cluster. At $(m - M)_0 = 18.2$ the cluster is aged 1.1 ± 0.2 Gyr; at $(m - M)_0 = 18.7$ it is 0.7 ± 0.2 Gyr. NGC 1783 is a sufficiently rich cluster that one can see the full development of red giants on the asymptotic giant branch from the M type, through S, to carbon rich atmospheres.

Subject headings: clusters: globular — galaxies: Magellanic Clouds — photometry — stars: evolution

I. INTRODUCTION

The Large Magellanic Cloud star cluster NGC 1783 has an absolute magnitude of $\sim M_v = -7.5$ and lies 3.8 kpc SW of the center of the LMC. The first photometric studies were by Sandage and Eggen (1960) and Gascoigne (1962), who noted the much greater red extent of the cluster's giant branch than was seen in Galactic globular clusters. That observation was later understood when Mould and Aaronson (1979) found a carbon star in NGC 1783 and explained that it was formed during the evolution of intermediate-mass stars up the asymptotic giant branch (AGB). The AGB was fully surveyed by Lloyd Evans (1980), allowing Mould and Aaronson (1982) to estimate the age of the cluster from the extent of the AGB as 4 ± 2 Gyr. NGC 1783 has a type V classification by Searle, Wilkinson, and Bagnuolo (1980), and lies in between the old and young disk rotation curves of Freeman, Illingworth, and Oemler (1983).

In this paper we present a deep color-magnitude diagram for NGC 1783 which permits its age to be estimated from the main-sequence turnoff. As shown in § III, the cluster is apparently a further member of the population of 1 to 3 billion yr clusters in the LMC.

II. THE COLOR MAGNITUDE DIAGRAM

We observed NGC 1783 at the du Pont telescope of the Las Campanas Observatory with the CHUEI reimaging CCD camera on 1983 October 9. Conditions were photometric, and the seeing was good, yielding images of 1″.4 FWHM. A total of 2500 s was accumulated in the red in four separate exposures, together with three 1000 s green frames (see Fig. 1 [Plate 2]). Two short exposures were also obtained.

The methods of picture processing and calibration (Nemec, Kristian, and Mould 1988) and photometry within the cluster (Jensen, Mould, and Reid 1988) have been described in two previous papers. Within 2′ of the cluster center 653 stars were automatically selected for photometry using the DAOPHOT program (Stetson 1987) with due regard for criteria such as image quality and freedom from contamination. These stars are identified in Figure 2 (Plates 3–4). Photometry of these stars on the Thuan and Gunn (1976) system is presented in Table 1 in the columns headed *R* and *G-R*. The columns headed *x* and *y* give the coordinates of these stars in pixel numbers with an origin at the bottom left of Figure 2*a* and a scale of 0.415″ pixel^{-1}. For comparison purposes photometry was also carried out in a subfield of equal size west of the cluster. To determine the relative efficiency of the program in finding stars in these two samples, artificial stars were inserted into the data with the same point spread function as was determined for the data itself. We found that the completeness was ~92% at 18th magnitude in the field sample, and ~52% in the cluster, falling to ~25% at 20th magnitude in the field, compared with ~17% in the cluster. The color-magnitude diagram for the stars in Table 1 is shown in Figure 3 after a field star subtraction procedure. The subtraction procedure allows field and cluster stars to mutually annihilate if they lie within 0.5 in magnitude and 0.1 in color of one another. This procedure is clearly only statistically valid and is an approximate one, since completeness is a function of radius in the cluster. The procedure is best regarded as equivalent to choosing in an unbiased way a subset of the cluster sample to represent the cluster color-magnitude diagram. We also cut off Figure 3 at $R > 21.5$, because of the low completeness and high probability of error due to confusion at this magnitude. Between $R = 18.5$ and $R = 21.5$ we required two field stars to eliminate one cluster star, and thus 439 field stars allowed us to represent NGC 1783 by 433 stars in Figure 3.

[1] Visiting Astronomers at Cerro Tololo Interamerican Observatory, a division of N.O.A.O., operated by AURA for the National Science Foundation.
[2] Deceased 1987 April 30.

© American Astronomical Society • Provided by the NASA Astrophysics Data System

1989ApJ...339...84M

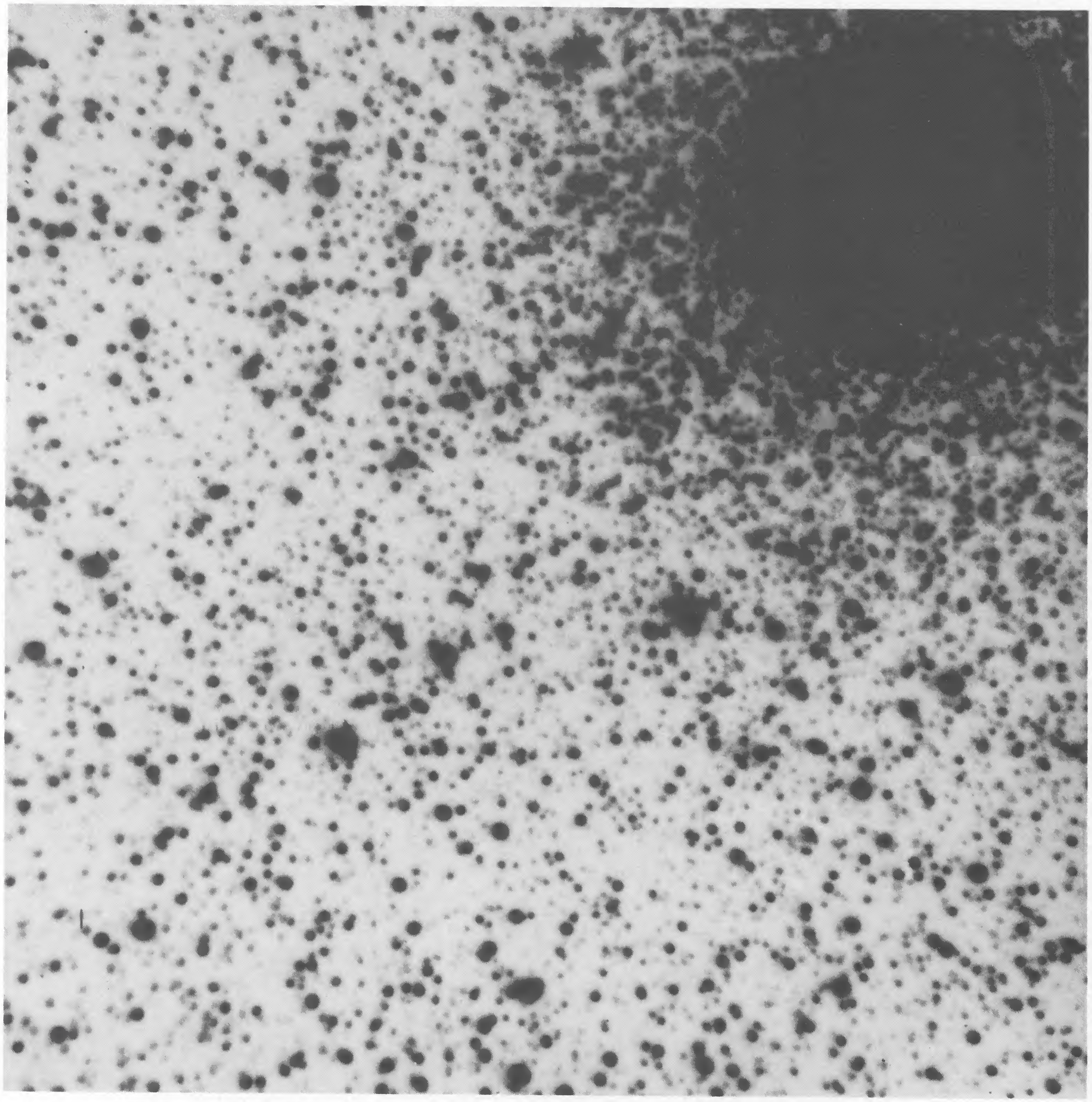

FIG. 1.—The accumulated green image of NGC 1783. North is up, and west is to the left. The limiting magnitude is $G = 23.7$.

© American Astronomical Society • Provided by the NASA Astrophysics Data System

1989ApJ...339...84M

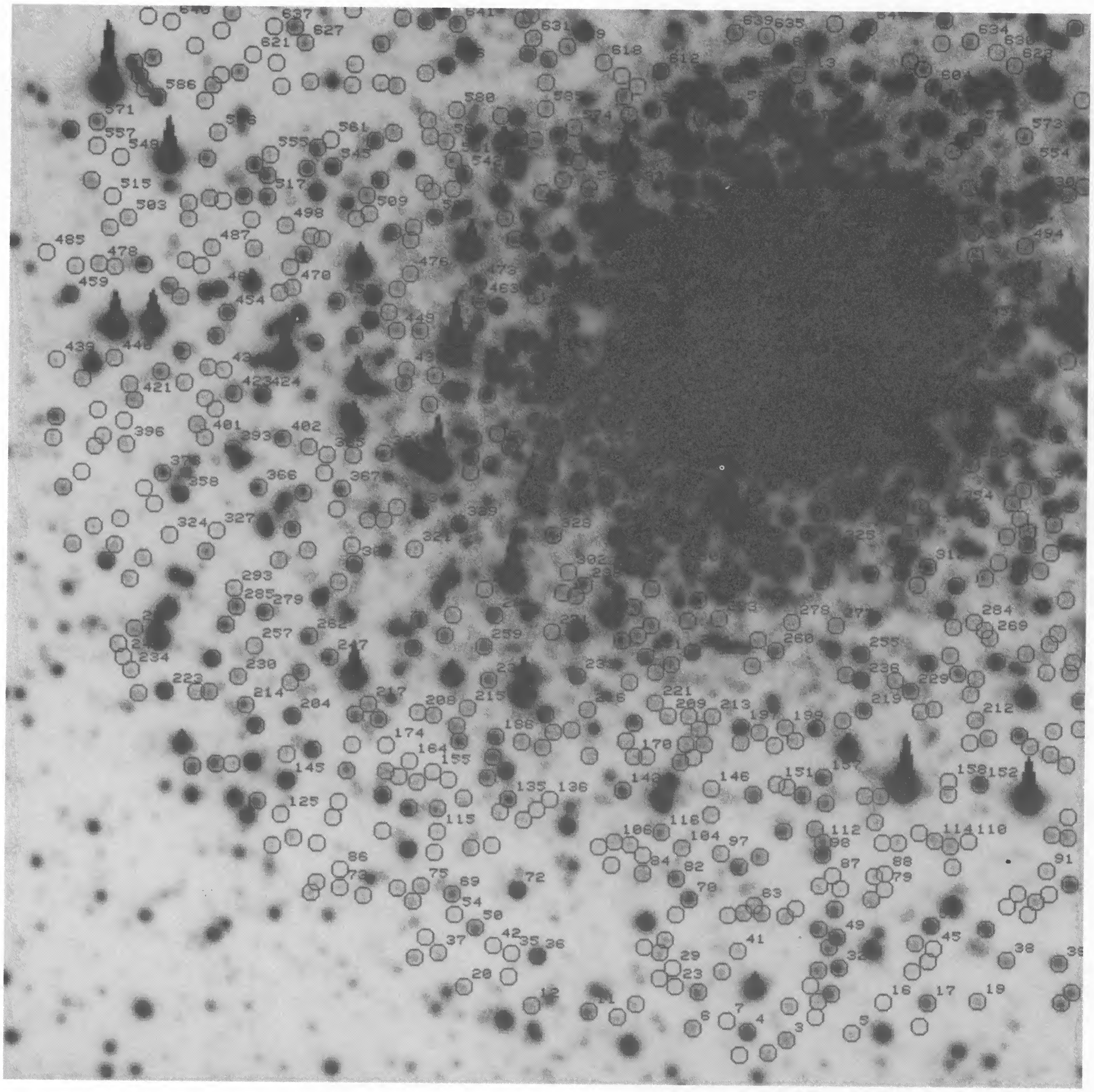

FIG. 2.—(*a*) Part of the averaged red frame of NGC 1783 is shown with stars from Table 1 identified. The star number is placed a constant distance above and to the right of the relevant box. Unlabeled stars can be identified from their relative (x, y) coordinates in the table. The orientation here is the same as Fig. 1. The limiting magnitude is $R = 23.5$.

MOULD *et al.* (*see* **339**, 84)

© American Astronomical Society • Provided by the NASA Astrophysics Data System

1989ApJ...339...84M

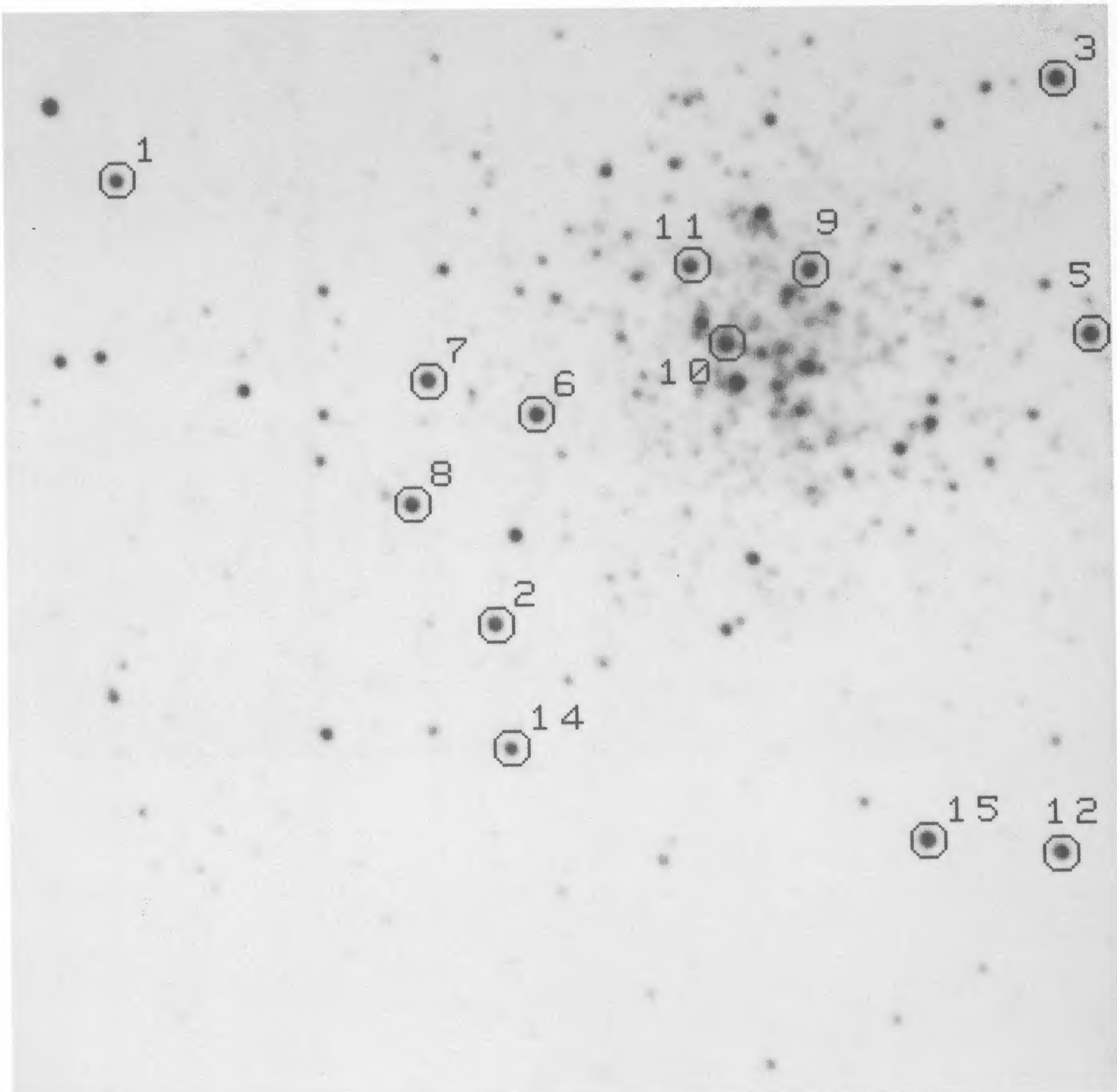

FIG. 2.—(*b*) The averaged red frame of NGC 1783 is shown with stars from Table 2 identified. The orientation here is the same as Fig. 1.

MOULD *et al.* (*see* **339**, 84)

© American Astronomical Society • Provided by the NASA Astrophysics Data System

TABLE 1

PHOTOMETRY OF NGC 1783

Star	x	y	R	$G-R$	Star	x	y	R	$G-R$	Star	x	y	R	$G-R$	Star	x	y	R	$G-R$
1	369	396	21.20	-0.18	49	406	442	18.68	0.34	97	361	474	20.89	-0.04	145	194	500	17.92	0.39
2	380	397	20.26	-0.19	50	267	444	18.98	0.28	98	400	474	18.66	0.19	146	357	499	20.66	-0.18
3	387	402	19.76	-0.43	51	399	445	18.86	0.43	99	241	474	17.79	0.45	147	244	500	20.58	-0.22
4	372	405	18.34	0.45	52	463	446	18.57	0.18	100	189	475	20.47	-0.11	148	256	501	21.33	-0.04
5	412	405	20.56	-0.42	53	442	447	18.48	0.35	101	206	476	21.16	-0.05	149	386	500	20.71	-0.07
6	351	406	19.93	-0.15	54	259	449	20.86	-0.09	102	273	476	20.71	-0.14	150	271	502	19.18	0.18
7	364	409	21.37	0.14	55	344	450	21.42	-0.37	103	314	476	21.38	-0.30	151	382	501	20.98	-0.27
8	438	408	21.21	-0.19	56	364	450	21.48	-0.27	104	346	476	20.49	-0.09	152	460	502	18.43	0.34
9	322	410	20.49	0.02	57	386	450	20.19	-0.19	105	197	478	20.22	0.35	153	237	502	20.64	-0.16
10	398	411	21.31	0.08	58	370	451	20.13	-0.23	106	320	478	20.67	-0.22	154	217	504	19.27	0.32
11	311	412	19.02	0.43	59	377	451	19.73	-0.23	107	326	477	20.47	-0.14	155	250	504	20.89	0.07
12	289	414	19.99	-0.24	60	479	452	21.11	-0.38	108	449	478	19.80	-0.49	156	278	505	17.96	0.41
13	329	415	20.78	-0.14	61	405	453	18.93	0.44	109	423	479	21.07	0.00	157	400	504	18.85	0.22
14	388	415	20.39	-0.18	62	243	454	20.19	-0.33	110	456	480	21.19	-0.26	158	448	503	21.28	-0.09
15	399	417	20.34	-0.17	63	374	454	20.30	-0.27	111	231	481	21.00	-0.03	159	158	505	18.88	0.35
16	424	417	22.55	-0.58	64	390	453	21.05	-0.13	112	400	479	19.27	-0.25	160	232	504	20.03	0.34
17	441	417	18.86	0.35	65	471	455	21.45	-0.20	113	429	479	20.66	-0.31	161	167	506	18.91	0.34
18	492	418	19.19	-0.54	66	224	456	20.62	-0.21	114	443	480	20.34	-0.31	162	173	506	20.72	-0.31
19	460	418	20.25	-0.30	67	419	457	20.22	-0.24	115	252	481	20.83	-0.14	163	181	507	17.70	0.22
20	263	421	19.91	0.13	68	204	457	20.45	-0.25	116	338	482	19.36	0.52	164	241	508	21.30	-0.15
21	353	420	19.15	0.42	69	258	457	19.08	0.35	117	437	483	21.07	-0.39	165	345	509	19.51	-0.06
22	404	420	18.89	0.36	70	349	456	18.73	0.43	118	494	482	19.85	-0.29	166	273	510	19.19	-0.37
23	344	422	21.44	-0.22	71	482	457	20.14	-0.24	119	385	483	18.82	0.33	167	493	510	20.57	-0.31
24	496	422	19.07	-0.60	72	283	459	17.84	0.47	120	488	483	20.23	-0.30	168	194	510	20.47	-0.17
25	396	423	21.20	-0.15	73	215	459	20.50	-0.45	121	397	484	19.63	-0.24	169	310	511	20.91	-0.10
26	280	425	21.19	0.05	74	237	459	20.44	-0.09	122	212	486	21.26	-0.08	170	327	511	20.97	-0.14
27	338	425	21.12	-0.12	75	246	460	20.20	-0.14	123	241	490	18.55	0.48	171	332	511	20.75	-0.22
28	362	428	20.30	-0.08	76	487	460	21.41	-0.24	124	285	486	20.83	0.03	172	350	511	21.14	-0.42
29	343	429	22.01	0.36	77	206	461	20.68	-0.11	125	192	487	20.63	-0.10	173	204	512	18.11	0.52
30	399	429	19.38	0.41	78	407	461	21.06	-0.38	126	420	487	20.36	-0.16	174	232	514	22.10	0.20
31	435	429	20.79	-0.14	79	424	461	21.04	-0.16	127	276	489	20.51	-0.10	175	219	514	21.02	-0.45
32	407	430	18.74	0.36	80	475	460	21.04	-0.15	128	252	490	19.45	-0.35	176	292	514	19.74	-0.39
33	244	432	20.15	-0.41	81	399	462	20.65	-0.24	129	290	490	21.30	0.07	177	487	514	20.24	-0.28
34	441	433	21.02	-0.42	82	344	464	19.05	0.32	130	357	489	20.50	-0.15	178	260	516	18.94	0.29
35	281	434	21.20	-0.01	83	495	464	18.72	0.38	131	494	490	21.10	-0.18	179	284	516	20.13	-0.16
36	291	433	18.17	0.59	84	331	466	19.94	-0.21	132	183	492	18.94	0.39	180	347	516	20.21	-0.12
37	253	434	20.42	-0.19	85	420	466	20.96	-0.21	133	214	492	21.15	-0.25	181	354	516	19.82	0.35
38	471	434	19.61	-0.29	86	215	466	21.56	-0.06	134	262	494	20.57	-0.17	182	368	517	20.28	0.07
39	491	433	18.89	0.31	87	404	466	21.23	-0.22	135	279	494	18.92	0.38	183	381	516	21.03	-0.20
40	338	435	20.23	-0.12	88	424	467	21.40	-0.37	136	295	494	21.31	0.13	184	324	517	21.18	-0.34
41	368	436	20.73	-0.24	89	319	469	21.03	-0.27	137	401	494	19.26	-0.05	185	479	517	20.50	-0.34
42	274	437	21.19	-0.03	90	368	469	18.77	0.33	138	231	495	18.29	0.35	186	274	518	18.64	0.47
43	332	437	21.11	-0.23	91	486	469	20.79	-0.16	139	373	497	18.88	0.19	187	389	518	20.92	-0.35
44	403	438	19.33	0.27	92	450	470	20.74	-0.14	140	392	497	18.92	0.27	188	456	518	21.39	-0.33
45	443	438	21.50	-0.21	93	265	475	20.05	-0.52	141	422	497	19.59	-0.02	189	296	520	20.64	-0.21
46	248	440	21.14	-0.22	94	251	473	21.25	0.14	142	323	498	18.88	0.46	190	463	520	19.94	0.13
47	340	440	20.38	0.37	95	331	473	21.20	-0.04	143	416	497	20.46	-0.32	191	182	521	18.20	0.47
48	436	440	20.03	0.04	96	376	473	19.40	0.27	144	448	498	20.52	-0.12	192	220	526	19.06	0.28

© American Astronomical Society • Provided by the NASA Astrophysics Data System

TABLE 1—*Continued*

Star	x	y	R	$G-R$
193	303	521	20.52	-0.41
194	375	521	20.18	-0.13
195	259	522	19.53	-0.20
196	352	522	20.20	0.25
197	368	523	18.23	0.53
198	475	521	18.91	0.37
199	385	523	20.11	-0.03
200	397	523	18.36	0.54
201	488	523	20.62	-0.23
202	229	524	18.95	0.34
203	498	524	20.90	-0.17
204	196	525	18.29	0.51
205	327	524	18.81	0.41
206	250	526	20.16	-0.12
207	293	527	18.62	0.16
208	244	527	21.45	-0.21
209	340	527	20.75	-0.05
210	348	527	20.99	-0.11
211	407	526	20.06	-0.20
212	458	527	20.58	-0.22
213	357	527	20.73	-0.15
214	178	529	19.23	0.27
215	263	529	20.40	-0.17
216	309	529	20.33	-0.27
217	225	530	19.66	-0.06
218	437	530	20.74	-0.30
219	415	530	18.86	0.50
220	442	531	20.62	-0.18
221	335	532	20.42	-0.34
222	137	533	20.04	-0.28
223	147	534	18.00	0.48
224	159	534	20.29	-0.47
225	164	534	19.62	-0.39
226	498	535	19.15	0.27
227	195	538	20.33	-0.51
228	456	537	20.82	-0.17
229	433	538	18.77	0.37
230	175	540	19.92	0.08
231	271	540	19.43	-0.49
232	325	540	20.79	-0.55
233	305	542	18.91	0.14
234	134	542	20.36	-0.13
235	199	542	19.07	-0.45
236	414	542	18.27	0.51
237	427	542	20.30	0.01
238	335	544	20.64	-0.28
239	408	544	19.93	-0.06
240	458	543	20.28	-0.06
241	451	545	19.25	0.23
242	485	546	21.24	0.19
243	494	546	20.15	-0.16
244	131	547	20.67	-0.20
245	165	547	17.99	0.30
246	341	547	19.70	-0.22
247	210	548	18.78	0.40
248	372	547	19.95	0.12
249	440	549	17.86	0.59
250	466	550	17.88	0.47
251	331	550	18.88	0.36
252	495	550	20.83	0.00
253	129	552	20.42	-0.23
254	349	552	18.94	0.43
255	414	552	18.56	0.34
256	448	552	20.40	-0.03
257	181	552	20.77	-0.26
258	242	552	18.76	0.30
259	269	553	19.14	0.57
260	381	553	19.12	-0.50
261	477	553	20.08	-0.16
262	202	556	18.78	0.26
263	322	556	19.24	0.54
264	254	557	19.45	-0.33
265	374	557	19.98	-0.01
266	135	558	19.65	0.29
267	328	558	19.76	-0.07
268	486	557	20.55	-0.27
269	463	559	20.39	-0.33
270	170	560	18.91	0.39
271	295	559	20.95	-0.22
272	333	562	20.07	-0.52
273	449	563	21.08	-0.23
274	461	562	20.64	-0.20
275	489	561	21.07	0.03
276	244	563	18.76	0.32
277	404	563	20.18	-0.13
278	387	564	21.07	0.75
279	185	565	18.81	0.32
280	257	565	21.18	0.08
281	273	565	18.75	0.47
282	347	564	20.84	-0.11
283	359	565	20.58	-0.05
284	457	565	20.79	-0.27
285	174	567	18.98	0.34
286	206	571	18.06	0.41
287	326	569	19.83	-0.13
288	304	573	20.03	-0.08
289	351	572	18.95	0.55
290	299	574	20.36	-0.22
291	382	574	17.81	0.15
292	492	574	21.02	0.15
293	173	574	20.63	-0.22
294	269	575	20.86	-0.27
295	333	576	20.70	1.19
296	133	577	20.17	0.19
297	213	577	20.41	-0.20
298	307	577	19.19	0.32
299	435	579	20.17	-0.25
300	450	579	18.77	0.38
301	398	580	19.43	-0.07
302	301	582	21.28	-0.29
303	461	582	19.76	-0.25
304	474	583	18.43	0.15
305	124	584	18.00	0.53
306	417	583	18.43	0.50
307	219	584	18.78	0.26
308	348	584	18.81	0.34
309	429	584	18.54	0.26
310	138	585	20.26	-0.16
311	190	585	20.05	-0.02
312	439	586	19.28	0.40
313	482	585	20.38	-0.32
314	162	588	19.54	-0.37
315	466	588	20.53	-0.11
316	400	589	17.81	-0.08
317	430	590	17.80	0.49
318	111	590	20.05	-0.04
319	127	590	20.27	-0.06
320	201	589	20.84	0.00
321	242	590	21.06	0.18
322	218	591	21.20	-0.14
323	486	592	21.20	-0.46
324	148	594	20.86	-0.12
325	404	593	17.86	0.27
326	477	595	19.09	0.21
327	166	596	20.98	-0.15
328	295	596	19.15	-0.07
329	427	595	18.74	0.36
330	492	596	18.57	0.51
331	119	597	20.60	-0.01
332	195	597	18.86	0.47
333	393	598	18.83	0.52
334	337	600	19.74	-0.02
335	432	599	19.66	-0.08
336	469	598	20.51	-0.25
337	487	603	20.03	-0.26
338	129	600	20.70	-0.17
339	259	600	18.54	0.18
340	224	601	20.57	-0.09
341	230	601	20.03	-0.10
342	477	600	19.84	-0.19
343	342	604	17.83	0.43
344	427	605	19.39	0.00
345	212	605	21.39	-0.20
346	244	605	18.25	0.41
347	322	605	19.60	1.20
348	459	605	18.80	0.52
349	474	605	21.13	0.93
350	142	606	21.38	-0.21
351	398	606	18.24	0.32
352	235	606	21.25	0.02
353	422	607	18.63	0.62
354	449	609	18.67	0.31
355	436	609	21.32	-0.11
356	455	609	18.71	0.21
357	486	609	18.10	0.35
358	152	610	17.88	0.51
359	315	611	18.66	0.52
360	344	611	19.27	0.52
361	471	611	20.06	0.17
362	493	611	18.74	0.29
363	107	612	19.54	0.45
364	138	612	21.76	0.36
365	199	611	19.04	-0.29
366	182	613	18.76	0.38
367	214	613	19.12	0.45
368	399	613	20.03	0.01
369	406	613	18.76	0.24
370	475	616	20.02	-0.26
371	315	616	19.11	0.49
372	362	615	18.25	0.56
373	114	618	21.45	-0.18
374	337	617	19.03	0.50
375	430	618	18.89	0.48
376	442	619	17.91	0.57
377	484	618	18.67	0.33
378	145	618	18.80	0.36
379	263	620	20.84	-0.04
380	305	618	17.90	0.52
381	207	619	21.47	0.06
382	326	619	17.88	0.23
383	271	623	19.05	0.41
384	419	622	18.75	0.81

© American Astronomical Society • Provided by the NASA Astrophysics Data System

TABLE 1—*Continued*

Star	x	y	R	$G-R$
385	208	626	21.06	-0.12
386	218	626	20.81	-0.69
387	263	626	18.76	0.34
388	331	626	17.98	0.35
389	455	626	20.40	0.13
390	119	628	20.84	-0.25
391	230	627	19.30	0.38
392	355	627	18.49	0.42
393	172	628	18.52	0.33
394	201	629	19.92	-0.07
395	278	630	19.27	0.21
396	131	629	20.35	-0.18
397	311	630	19.22	0.53
398	414	631	18.26	0.31
399	103	631	20.40	-0.24
400	122	632	20.41	-0.12
401	161	632	20.54	-0.30
402	191	632	18.88	0.37
403	295	632	18.33	0.38
404	339	632	18.65	0.51
405	291	633	19.37	-0.02
406	473	633	18.47	-0.57
407	264	633	18.90	0.23
408	280	633	19.29	0.25
409	273	635	20.24	-0.15
410	370	636	18.13	0.22
411	158	637	19.86	-0.18
412	130	638	21.39	-0.11
413	294	638	18.52	0.30
414	488	638	18.64	0.30
415	104	639	18.82	0.35
416	288	640	20.12	-0.60
417	120	642	21.21	-0.01
418	315	642	18.15	0.25
419	165	643	21.21	-0.14
420	247	646	20.24	-0.33
421	134	646	19.52	-0.11
422	161	647	21.01	-0.34
423	172	649	18.85	0.31
424	183	649	18.14	0.50
425	269	650	19.20	0.52
426	284	650	18.73	0.30
427	132	652	20.08	-0.31
428	114	654	20.17	-0.02
429	153	653	20.81	-0.29
430	237	654	19.82	0.21
431	311	656	18.54	0.25
432	144	657	19.45	0.18
433	249	657	20.12	-0.03
434	168	658	21.01	-0.10
435	282	658	19.01	1.11
436	447	659	17.83	0.69
437	162	659	20.27	0.11
438	238	659	20.30	0.24
439	104	661	20.61	-0.20
440	126	662	20.40	-0.09
441	453	662	19.28	1.05
442	152	665	18.76	0.35
443	491	666	20.70	-0.05
444	457	667	19.91	0.23
445	203	669	18.55	0.35
446	165	671	18.82	0.42
447	218	672	18.71	0.48
448	325	672	18.96	0.48
449	234	674	19.99	-0.01
450	243	674	19.65	-0.01
451	328	677	18.16	0.63
452	453	676	18.34	0.36
453	224	678	17.76	0.63
454	169	680	18.82	0.36
455	458	680	18.69	0.67
456	231	681	20.25	0.08
457	273	684	18.02	0.62
458	211	685	18.77	0.45
459	109	686	18.24	0.47
460	151	686	19.85	-0.18
461	332	686	18.65	1.53
462	189	688	20.79	-0.02
463	266	686	19.33	-0.10
464	287	688	20.20	-0.19
465	311	688	18.08	0.54
466	161	688	18.54	0.25
467	166	689	18.20	0.29
468	342	688	18.54	0.65
469	147	690	19.30	0.15
470	194	690	20.28	-0.14
471	234	690	20.25	-0.08
472	284	692	18.49	0.27
473	265	693	18.68	0.43
474	419	694	18.52	1.38
475	126	697	20.42	-0.08
476	239	696	20.51	0.11
477	111	697	20.77	-0.20
478	120	698	20.12	-0.21
479	159	698	21.03	-0.02
480	193	698	21.05	-0.12
481	467	698	18.65	0.38
482	137	698	18.69	0.38
483	153	700	20.48	-0.13
484	457	701	18.80	0.60
485	100	702	21.23	-0.18
486	198	703	18.91	0.41
487	163	705	20.49	-0.09
488	179	705	20.36	-0.44
489	455	706	20.49	-0.06
490	205	709	20.89	-0.12
491	239	709	20.07	-0.47
492	201	710	20.67	-0.06
493	279	710	19.60	0.52
494	474	710	20.52	-0.14
495	124	712	20.21	0.05
496	232	712	18.68	0.41
497	454	715	20.66	-0.40
498	191	714	21.10	-0.21
499	240	714	20.16	-0.13
500	154	716	20.29	-0.22
501	178	716	21.08	-0.16
502	461	716	19.91	-0.53
503	131	716	20.40	-0.14
504	218	717	20.71	-0.22
505	275	718	20.37	0.51
506	424	718	20.00	-1.23
507	248	718	18.86	0.38
508	284	719	18.78	0.24
509	223	719	20.98	-0.07
510	475	720	19.43	0.13
511	154	722	20.45	-0.19
512	454	722	18.51	0.23
513	479	722	18.71	0.35
514	167	723	21.66	-0.33
515	125	724	21.34	-0.27
516	162	724	20.08	0.45
517	184	725	18.89	0.39
518	175	725	18.79	0.34
519	222	726	19.72	-0.22
520	294	726	18.65	0.12
521	459	730	18.58	0.58
522	474	726	18.37	0.46
523	203	727	17.78	0.46
524	247	728	20.20	-0.05
525	468	728	18.56	0.71
526	255	729	20.59	-0.05
527	289	728	20.43	0.04
528	117	730	19.75	-0.41
529	307	730	20.41	0.00
530	478	730	17.91	0.54
531	490	730	19.35	-0.05
532	244	731	21.24	-0.30
533	321	730	18.06	0.31
534	423	732	18.47	0.50
535	452	732	20.25	-0.19
536	354	732	19.79	0.34
537	496	733	19.92	-0.27
538	184	733	18.81	0.40
539	227	732	18.81	0.36
540	297	733	20.21	-0.03
541	429	732	18.67	0.20
542	259	735	18.54	0.11
543	199	736	18.97	0.40
544	433	736	19.05	0.09
545	209	737	18.50	0.25
546	460	737	18.88	0.69
547	179	737	18.79	0.38
548	128	739	21.22	-0.19
549	237	740	17.91	0.58
550	161	739	19.21	0.55
551	255	740	20.14	-0.20
552	303	740	20.37	-0.30
553	439	740	19.32	0.50
554	476	741	18.70	0.52
555	185	741	20.87	-0.16
556	298	742	18.69	0.38
557	119	743	20.79	-0.16
558	203	744	18.84	0.26
559	246	749	20.84	-0.42
560	446	746	21.46	-0.27
561	208	747	20.47	0.25
562	225	747	18.65	-0.50
563	252	747	19.78	0.37
564	109	749	18.09	0.54
565	286	748	20.01	-0.25
566	165	749	20.48	-0.46
567	280	749	18.54	0.40
568	232	750	20.09	-0.54
569	295	750	18.80	0.48
570	450	750	19.15	0.43
571	119	752	19.13	0.29
572	382	753	18.68	0.44
573	473	752	20.08	0.04
574	301	753	20.18	-0.06
575	388	754	18.36	0.57
576	245	755	20.18	-0.29

© American Astronomical Society • Provided by the NASA Astrophysics Data System

1989ApJ...339...84M

TABLE 1—*Continued*

Star	x	y	R	$G-R$	Star	x	y	R	$G-R$
577	455	755	18.88	0.87	616	252	776	18.27	0.45
578	273	757	20.12	-0.01	617	140	777	19.22	0.38
579	350	757	20.72	-0.38	618	312	778	20.46	-0.22
580	256	759	20.52	-0.04	619	434	777	19.40	0.91
581	322	758	19.89	0.04	620	291	779	19.17	0.10
582	357	759	18.01	0.27	621	178	779	21.40	-0.02
583	331	760	18.55	0.53	622	429	780	19.81	0.38
584	160	761	20.69	-0.27	623	469	779	19.75	0.33
585	290	760	20.84	-0.11	624	283	781	18.81	0.43
586	142	762	18.41	0.45	625	156	782	21.01	-0.11
587	364	761	18.99	0.46	626	381	782	17.37	0.44
588	449	763	19.60	0.19	627	198	784	19.45	0.48
589	137	765	19.12	0.29	628	227	784	19.39	-0.47
590	320	765	20.12	0.12	629	298	784	19.84	-0.45
591	389	765	19.22	0.53	630	462	784	21.06	1.05
592	444	766	19.00	0.69	631	285	787	20.15	-0.04
593	163	767	19.65	-0.52	632	441	787	20.47	0.34
594	189	767	20.91	-0.51	633	166	788	21.35	-0.29
595	495	766	21.32	-0.29	634	452	788	19.69	0.27
596	216	768	20.49	-0.09	635	374	789	21.24	0.41
597	200	769	20.31	-0.05	636	410	790	18.73	0.32
598	227	769	20.74	-0.24	637	186	790	21.07	-0.14
599	233	768	19.94	-0.24	638	194	790	18.99	0.14
600	325	769	21.03	-0.02	639	362	790	19.59	-0.12
601	403	769	18.80	0.56	640	147	791	20.94	-0.33
602	135	770	18.61	0.31	641	256	792	19.10	-0.45
603	290	770	20.74	0.34	642	138	793	21.34	0.15
604	438	770	18.79	0.71	643	244	793	18.86	-0.01
605	166	771	20.70	-0.16	644	281	794	19.69	-0.41
606	428	772	17.76	0.74	645	235	794	19.95	-0.15
607	173	772	19.49	0.42	646	400	794	20.65	-0.30
608	244	773	20.56	0.01	647	413	793	19.01	0.35
609	319	773	22.17	0.50	648	492	794	19.01	0.25
610	361	774	18.95	0.41	649	170	795	19.69	-0.17
611	133	775	18.55	0.33	650	442	796	19.07	0.58
612	334	775	18.62	0.36	651	216	797	20.78	-0.18
613	386	774	19.90	0.04	652	250	797	18.13	0.33
614	187	776	21.21	-0.04	653	284	796	19.77	-0.06
615	217	776	20.89	-0.15					

A check of the photometric zero points was carried out by identifying 32 stars in common with Gascoigne (1962). Gunn magnitudes were predicted from Gascoigne's photographic magnitudes by means of the transformations described in the next section. After rejection of 2 σ residuals (probably mostly misidentifications) the difference between predicted and observed G-R was 0.02 ± 0.04 mag and the difference between predicted and observed R was -0.01 ± 0.03 mag.

Stars brighter than $R = 17.5$ are not included in Table 1 because their images are saturated on the red frames. We compared the photometry of stars in the next half magnitude to $R = 18$ between the long and short exposures. The magnitude difference was found to be identical to that obtained for a sample of stars at $R = 19$. The photometry in Table 1 is therefore free from any CCD saturation problems.

III. THE AGE OF THE CLUSTER

To fit isochrones and determine the age of the cluster, we need first to determine the reddening, metallicity, and distance modulus. The reddening maps of Burstein and Heiles (1982), based on H I data for the Galaxy, show $E(B-V)$ between 0.03 and 0.06 in the direction of N1783. The H I map of the Magellanic system by Mathewson and Ford (1983) shows N1783 superposed on a region of high H I column density with a value of $\sim 10^{21}$ atoms cm^{-2} at the position of the cluster. This corresponds to an additional possible reddening of $E(B-V) = 0.04$, if the calibration of Burstein and Heiles is appropriate. The cluster would therefore seem to be reddened by between 0.03 and 0.10 in $E(B-V)$.

The metallicity of NGC 1783 has been determined by Cohen (1982), who finds $[M/H] = -0.45 \pm 0.3$. We can check this by means of the color of the giant branch at the luminosity of the horizontal branch, which is $0.42 < (G-R)_{0,g} < 0.57$ from Figure 3 with allowance for the reddening uncertainty. This corresponds to $-1.0 < [M/H] < -0.5$, if the age is close to 2 Gyr (see Da Costa, Mould, and Crawford 1985 [hereafter DMC] for details of the calibration). A correction to [M/H] of approximately $+0.2$ dex is required for an age of 1 Gyr according to the Yale isochrones, indicating consistency with the spectroscopic determination.

Superposed on Figure 3*a* and 3*b* are Vandenberg (1985) isochrones for $Z = 0.006$ for a distance modulus $(m - M)_0 = 18.2$ and reddenings of $E(B-V) = 0.03$ and 0.10. We have referred to this value of the distance as the *short modulus* in previous papers on this subject. DMC and Rich, Da Costa, and Mould (1984) discuss the distance modulus uncertainty for the

© American Astronomical Society • Provided by the NASA Astrophysics Data System

1989ApJ...339...84M

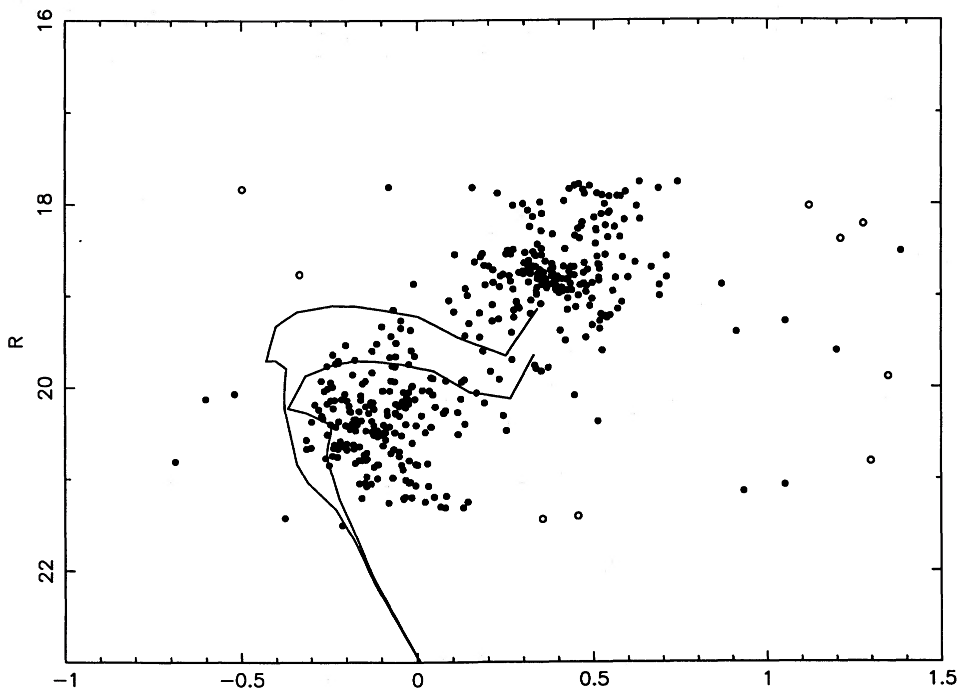

FIG. 3a

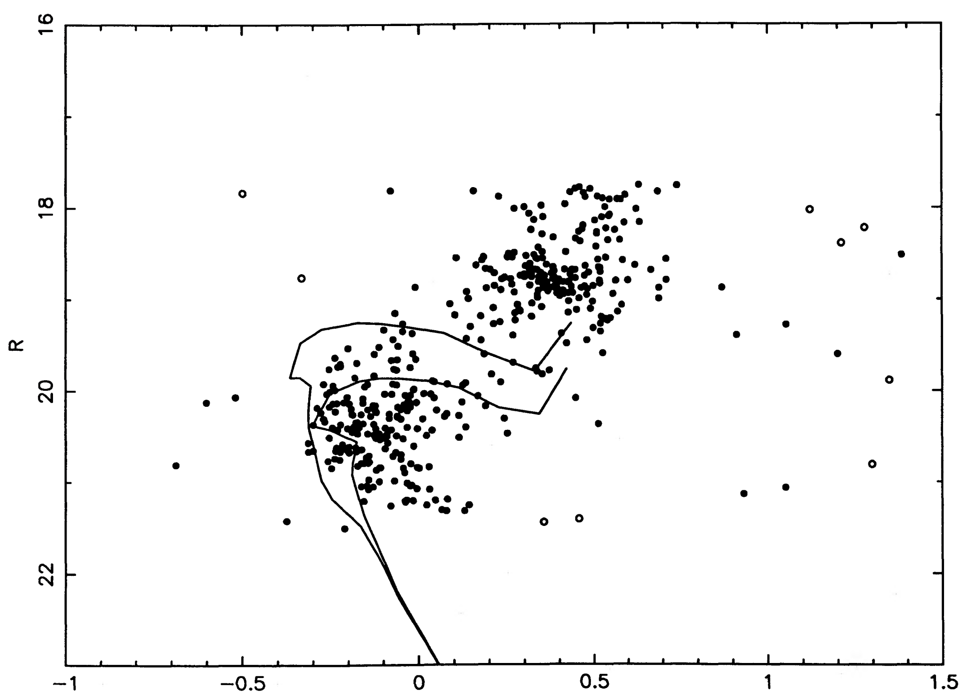

FIG. 3b

FIG. 3.—(a) A color magnitude diagram for NGC 1783 from the data of Table 1. Isochrones of $Z = 0.006$ and ages 0.8 and 1.25 Gyr are superposed at $(m - M)_0 = 18.2$. A reddening equivalent to $E(B-V) = 0.03$ is assumed. Open circles indicate stars which have been "oversubtracted" by the field subtraction procedure described in the text. In (b) everything is the same except the isochrones are reddened by $E(B-V) = 0.10$.

© American Astronomical Society • Provided by the NASA Astrophysics Data System

1989ApJ...339...84M

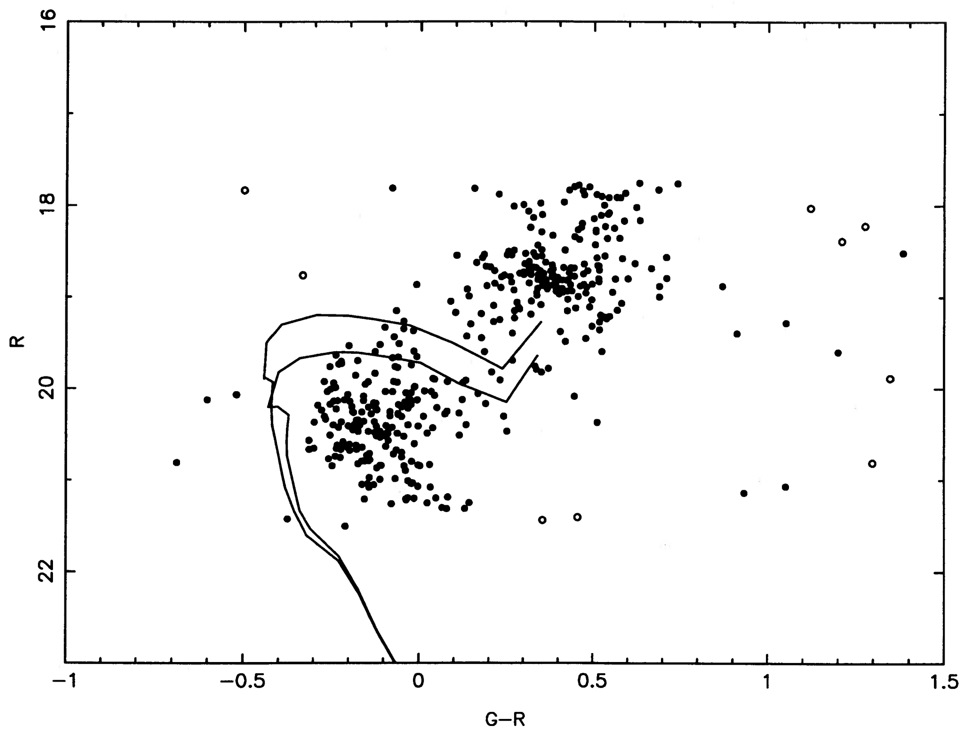

FIG. 4a

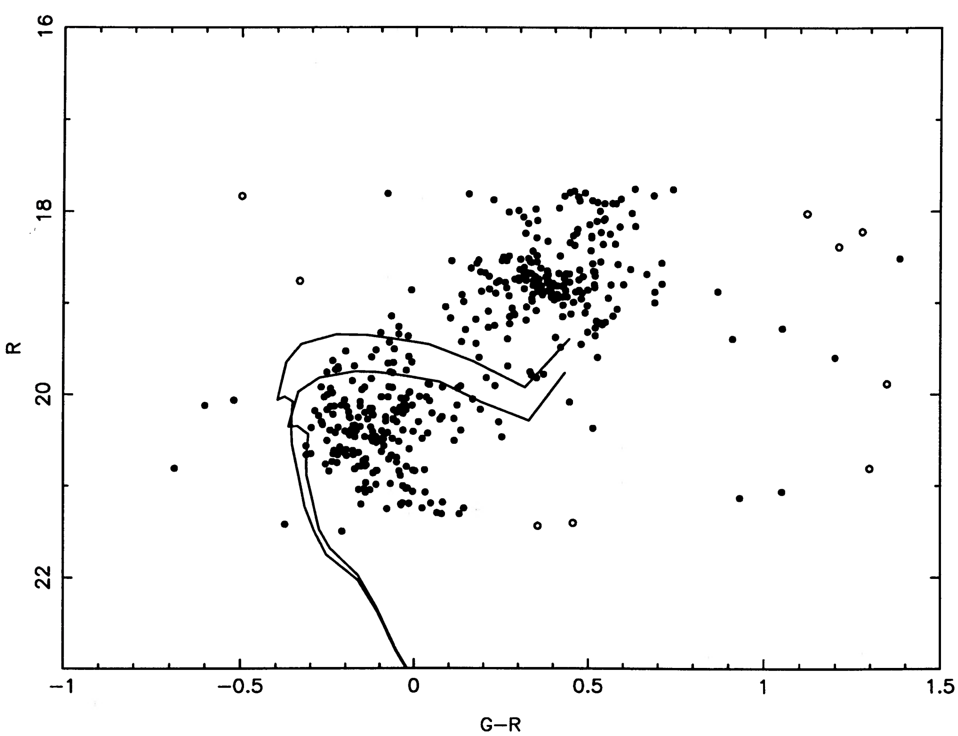

FIG. 4b

FIG. 4.—(a) The same color magnitude diagram for NGC 1783. Isochrones of $Z = 0.006$ and ages 0.6 and 0.8 Gyr are superposed at $(m - M)_0 = 18.7$. A reddening equivalent to $E(B-V) = 0.03$ is assumed. In (b) everything is the same except the isochrones are reddened by $E(B-V) = 0.10$.

© American Astronomical Society • Provided by the NASA Astrophysics Data System

1989ApJ...339...84M

Magellanic Clouds in more detail. The distance dichotomy relates to both the LMC and SMC. The Vandenberg isochrones have a helium content appropriate to the LMC of $Y = 0.25$. Transformations to the Gunn system are required for the Vandenberg isochrones. We took the relations given in Bell and Vandenberg (1986, Figs. 1 and 2) and interpolated them appropriately in metallicity. The isochrones are not a good fit to the data, comparing very unfavorably with the excellent fit that can be obtained by CCD photometry of less crowded fields (see Hesser *et al.* 1987 for 47 Tuc). In order to use them to evaluate the age of the cluster, one must attempt to isolate the tip of the main sequence and fit to that. The lower, 1.25 Gyr isochrone passes 0.4 to 0.6 mag fainter than five stars in Figure 3 in the range 19.1–19.4 in R and -0.1 to 0 in G-R. Most of these stars are likely to be cluster members, and thus represent the tip of the main sequence in NGC 1783 with an uncertainty of ~ 0.2 mag. Regardless of the quality of the fit and cluster membership, however, there are also systematic uncertainties to consider relating to the structure of stars exhausting their core hydrogen (Bertelli, Bressan, and Chiosi 1985). We treat this matter, following DMC, by allowing 0.3 mag of convective overshooting above the maximum main-sequence luminosity of this isochrone, and obtain an age estimate of 1.1 ± 0.2 Gyr for NGC 1783 at the short distance modulus.

Figure 4*a* and 4*b* show isochrones for the same chemical composition and ages of 0.6 and 0.8 Gyr superposed on the

TABLE 2

AGB Stars in NGC 1783

LE	$M_{\rm bol}$	Spectrum
1........	−5.35	C
2........	−4.5	S4/2
3........	−4.95	C
4........	−4.65	S5/2
5........	−4.55	M3
6........	−4.4	M3
7........	−4.2	M3
8........	−4.3	M3
9........	−4.8	S5/3
10........	−4.4	M4
11........	−4.3	...
15........	−4.1	M1

Sources.—For Identification: Lloyd Evans 1980. For Photometry: Frogel and Cohen 1983, Mould and Aaronson 1982, and Aaronson and Mould 1982. For Spectra: this paper; Lloyd Evans 1983, 1984; Bessell, Wood, and Lloyd Evans 1983; and Mould and Aaronson 1979.

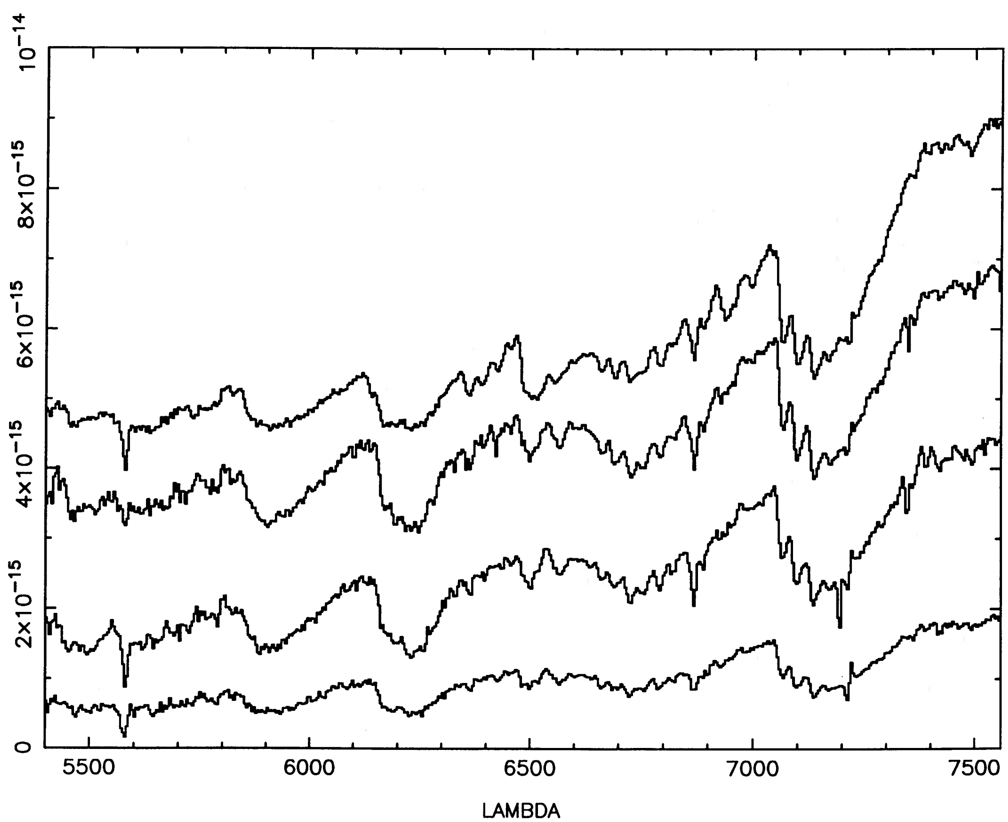

Fig. 5.—Spectra from top to bottom of LE 9, LE 10, LE 7, and LE 8. The wavelength scale is in angstroms and the vertical scale is in F_λ units. LE 9 and LE 10 were vertically offset by two and four vertical divisions respectively.

© American Astronomical Society • Provided by the NASA Astrophysics Data System

1989ApJ...339...84M

color-magnitude diagram at a larger assumed distance: $(m - M)_0 = 18.7$. The fit to the data is worse than for the short distance modulus in Figure 3*b*, but, following the arguments presented by Paczyński (1984), we should pay less attention to color discrepancies in isochrones than to the luminosity fit. With the same allowance for the effects of convective overshooting we obtain an age estimate of 0.7 ± 0.2 Gyr. The uncertainty in metallicity given by Cohen of 0.3 dex contributes to a further uncertainty of 0.1 Gyr in age. The tendency for isochrones to be bluer than the observed main sequence seems to be general in Magellanic Cloud clusters of ~ 1 Gyr, and independent of photometric system (see DMC, Mateo and Hodge 1987). This suggests the effect is real[3] rather than a transformation error.

IV. THE ASYMPTOTIC GIANT BRANCH

NGC 1783 is significantly younger than the other rich LMC clusters, whose AGB properties are discussed by Mould, Da Costa, and Wieland (1986). The AGB of NGC 1783 is well populated, as shown in Table 2, which summarizes our knowledge of its stellar content. The AGB is not seen in Figure 3; these stars are beyond the saturation limit of the long exposures. Spectra of four of these stars are shown in Figure 5, obtained with the RC spectrograph and GEC CCD detector at the 4 m telescope of the Cerro Tololo Inter-American Observatory. The spectra were obtained on 1982 November 25, and include two stars with no previously reported spectroscopy. Figure 5 illustrates the transition from M type to S type on the AGB. The ZrO band at 6472 Å is present also in the three (lower) M type spectra, but increases greatly in strength in the top spectrum of LE 9.

The AGB of NGC 1783 follows ideally the expectations from the theory of third dredge up (e.g., Iben and Renzini 1983). This was first noted by Bessell, Wood, and Lloyd Evans (1983), but can now be fully appreciated from the more complete data in Table 2. M stars populate the luminosity range $-4.5 < M_{\rm bol} < -4$ exclusively. The four S stars fall entirely in the range $-4.9 < M_{\rm bol} < -4.5$. And the brightest stars (-4.95 and -5.35) are both carbon stars.

Particularly noteworthy is the fact that the transition luminosity range, over which M stars turn into carbon stars through S stars on their way up the AGB is half a magnitude brighter in NGC 1783 than in the 2 Gyr clusters discussed by Mould, Da Costa, and Wieland. This supports a claim made by Lloyd Evans (1983, 1984), based on the integrated color classes of clusters. The result can be understood in terms of the higher luminosity at which more massive stars commence thermal pulsing on the AGB (e.g., Lattanzio 1987; Boothroyd and Sackmann 1988).

[3] An anonymous referee has suggested that an error in the envelope opacities used in calculating the models might be the source of this general problem. Color magnitude diagrams free of crowding noise will probably be required before this suggestion is entertained.

This work was supported in part by NSF grant AST 85-02518 and in part by a NASA contract to the HST Wide Field and Planetary Camera team.

REFERENCES

Aaronson, M., and Mould, J. 1982, *Ap. J. Suppl.*, **48**, 161.
Bell, R., and VandenBerg, D. 1986, *Ap. J. Suppl.*, **63**, 335.
Bertelli, G., Bressan, A., and Chiosi, C. 1985, *Astr. Ap.*, **150**, 33.
Bessell, M., Wood, P., and Lloyd Evans, T. 1983, *M.N.R.A.S.*, **202**, 59.
Boothroyd, A. I., and Sackmann, I.-J. 1988, *Ap. J.*, **238**, 671.
Burstein, D., and Heiles, C. 1982, *A.J.*, **87**, 1165.
Cohen, J. G. 1982, *Ap. J.*, **258**, 148.
Da Costa, G. S., Mould, J., and Crawford, M. 1985, *Ap. J.*, **297**, 582 (DMC).
Freeman, K., Illingworth, G., and Oemler, A. 1983, *Ap. J.*, **272**, 488.
Frogel, J., and Cohen, J. 1983, *Ap. J.*, **253**, 580.
Gascoigne, S. C. B. 1962, *M.N.R.A.S.*, **124**, 201.
Hesser, J., Harris, W., Vandenberg, D., Allwright, J., Shott, P., and Stetson, P. 1987, *Pub. A.S.P.*, **99**, 739.
Iben, I., Jr., and Renzini, A. 1983, *Ann. Rev. Astr. Ap.*, **21**, 271.
Jensen, J., Mould, J., and Reid, I. N. 1988, *Ap. J. Suppl.*, **67**, 77.
Lattanzio, J. C. 1987, *Ap. J. (Letters)*, **313**, L15.
Lloyd Evans, T. 1980, *M.N.R.A.S.*, **193**, 87.
———. 1983, *M.N.R.A.S.*, **204**, 975.
———. 1984, *M.N.R.A.S.*, **208**, 447.
Mateo, M., and Hodge, P. 1987, *Ap. J. Suppl.*, **60**, 893.
Mathewson, D. S., and Ford, V. 1983, in *Structure and Evolution of the Magellanic Clouds*, ed. S. van den Bergh and K. de Boer (Dordrecht: Reidel), p. 125.
Mould, J., and Aaronson, M. 1979, *Ap. J.*, **232**, 421.
———. 1982, *Ap. J.*, **263**, 629.
Mould, J. R., Da Costa, G. S., and Wieland, F. P. 1986, *Ap. J.*, **309**, 39.
Nemec, J., Kristian, J., and Mould, J. 1989, in preparation.
Paczyński, B. 1984, *Ap. J.*, **284**, 670.
Rich, R. M., Da Costa, G., and Mould, J. 1984, *Ap. J.*, **286**, 517.
Sandage, A., and Eggen, O. 1960, *M.N.R.A.S.*, **121**, 232.
Searle, L., Wilkinson, A., and Bagnuolo, W. 1980, *Ap. J.*, **239**, 803.
Stetson, P. 1987, *Pub. A.S.P.*, **99**, 191.
Thaun, T., and Gunn, J. E. 1976, *Pub. A.S.P.*, **88**, 543.
VandenBerg, D. 1985, *Ap. J. Suppl.*, **58**, 711.

JOSEPH JENSEN and JEREMY MOULD: Caltech 105–24, Pasadena CA 91125

JEROME KRISTIAN: M.W.L.C.O., 813 Santa Barbara St., Pasadena, CA 91101

JAMES NEMEC: Geophysics and Astronomy Department, University of British Columbia, Vancouver BC V6T 1W5, Canada

© American Astronomical Society • Provided by the NASA Astrophysics Data System